ELSEVIER

Engineering Geology 63 (2002) 233–245

ENGINEERING GEOLOGY

www.elsevier.com/locate/enggeo

Crack damage stress as a composite function of porosity and elastic matrix stiffness in dolomites and limestones

V. Palchik *, Y.H. Hatzor

Deichmann Rock Mechanics Laboratory of the Negev, Department of Geological and Environmental Sciences, Ben-Gurion University of the Negev, Beer-Sheba 84105, Israel

Received 19 June 2000; accepted 10 July 2001

Abstract

Twenty-five uniaxial compression tests were performed to determine stress at onset of dilation, referred to herein as "the crack damage stress," in heterogeneous dolomites and limestones. A simplified model for crack damage stress (σ_{cd}) is developed here using porosity, elastic modulus, Poisson's ratio and three empirical coefficients. The model shows that when porosity decreases and elastic modulus increases, σ_{cd} rapidly increases and approaches its maximum value. On the other hand, when porosity increases and elastic modulus decreases, σ_{cd} rapidly decreases and approaches its minimum value. The proposed model is validated for six heterogeneous limestone and dolomite formations which are widely distributed in Israel.

Keywords: Uniaxial compressive strength; Porosity; Dilation; Crack damage stress; Brittle fracture

1. Introduction

Relations between uniaxial compressive strength of heterogeneous rocks and porosity were reported for sandstones (Dunn et al., 1973; Hoshino, 1974; Vernik et al., 1993; Farquhar et al., 1994; Palchik, 1999), for granites and dolerites (Dearman et al., 1978; Lumb, 1983), for basalts (Al-Harthi et al., 1999), for dolomites (Hatzor and Palchik, 1998) and for limestones (Palchik and Hatzor, 2000). The general relation is that the uniaxial compressive strength decreases with increasing porosity. It is evident that in heterogeneous rocks, existing pores are significant stress concentrators and therefore strongly influence rock strength (e.g. Dunn et al., 1973; Logan, 1987; Scott and Nielson, 1991; Teufel and Rhett, 1991). Olsson (1974), Fredrich et al. (1990), and Wong et al. (1996) have reported good correlation between the inverse square root of mean grain size and ultimate strength. These tests, however, primarily concentrated on extremely homogeneous samples in which the only textural variable was the mean grain size. Hatzor and Palchik (1997) have shown in heterogeneous dolomites that grain boundaries function as initial Griffith flaws (Griffith, 1921; Bieniawski, 1967) only in the very restricted case of low porosity (3–4%) and small grain size (<10 μm).

* Corresponding author. Tel.: +972-8646-1770; fax: +972-8647-2997.

E-mail address: vplachek@bgumail.bgu.ac.il (V. Palchik).

0013-7952/02/$ - see front matter
PII: S0013-7952(01)00084-9

Palchik (1999) also showed that in porous heterogeneous sandstones, porosity has an effect on uniaxial compressive strength, whereas the role of grain boundaries is negligible. In that study, it was shown that the uniaxial compressive strength is a composite function of porosity and elastic modulus. Palchik and Hatzor (2000) have further shown in heterogeneous limestones that the role of grain to grain contact lengths and porosity may be more significant in strength prediction than the role of individual grain size.

The objective of this paper is to develop an empirical model to describe a characteristic and important stress level—"the crack damage stress," using porosity and elastic parameters obtained from tests performed on samples collected from six dolomite and limestone formations which are widely distributed in Israel. In the analysis, the treatment of mean grain size is avoided since it is believed to be less significant, (Hatzor et al., 1997; Palchik and Hatzor, 2000), and because it is quite difficult to measure. Porosity may be viewed as a bulk measure of the void space in the rock, consisting primarily of fissures, pores, and open cracks, which may function as stress concentrators. Elastic modulus is a measure of overall rock stiffness, including the stiffness of grain to grain contacts (length of grain to grain contacts and number of contacts per grain) and the intergranular matrix (Hatzor et al., 1997; David et al., 1998).

The crack damage stress, generally referred to as the stress at onset of dilation, is a true rock material property in rock mechanics. Until this stress level is attained, the rock volume decreases. When the crack damage stress is attained, the volume begins to increase (Bieniawski, 1967; Schock et al., 1973; Brace, 1978; Paterson, 1978; Brady and Brown, 1993). Martin and Chadler (1994) and Eberhardt et al. (1999) have used the term "crack damage stress σ_{cd}" and have shown that brittle rocks become critically damaged at σ_{cd}, which is significantly lower than the failure stress. The mechanical significance of σ_{cd}, therefore, is quite obvious. For example, once stress concentrations around underground openings exceed σ_{cd}, the permeability of the rock is expected to increase and in situ crack growth may ensue. Furthermore, the mechanical energy stored in a rock which has been stressed up to that level, may be sufficient in some cases to induce unstable fracture propagation.

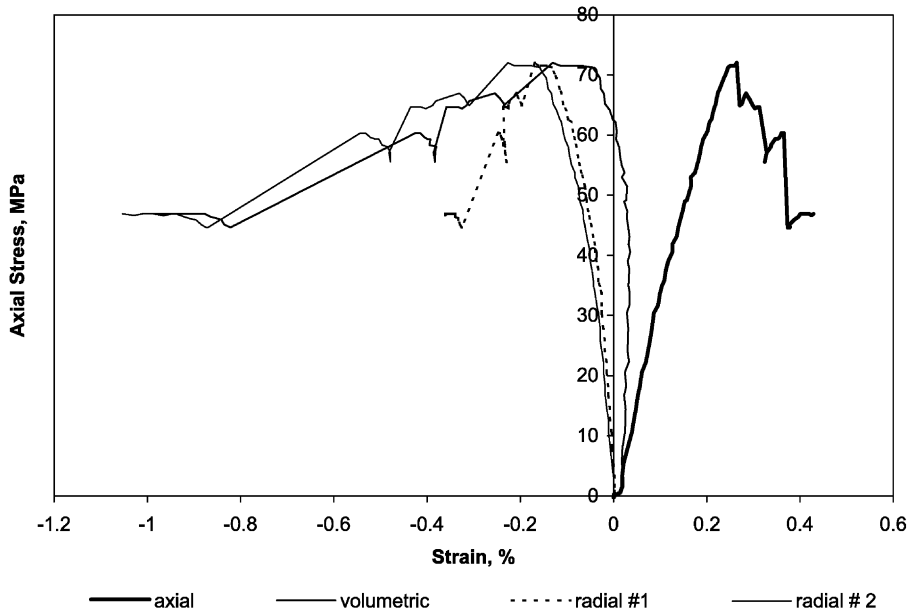

Fig. 1. Axial stress versus axial, radial and volumetric strains for Beit-Meir dolomite sample (BM-2).

2. Experimental programme

2.1. Specimen preparation

Twenty-five samples, including six of Bina Limestone, five of Aminadav Dolomite, three of Yagur Dolomite, three of Sorek Dolomite, six of Nekarot Limestone and two of Beit-Meir Dolomite (Israel), were tested under uniaxial compression. The samples were retrieved from depths of up to 300 m.

Specimen preparation and testing were performed in the Rock Mechanics Laboratory at Ben-Gurion University under strict adherence to ISRM and ASTM standards. The tests were performed on 54-mm-diameter solid cylinders with roughness smaller than 0.01 mm, perpendicularity smaller than 0.05 rad, and L/D ratio of approximately 2.0.

2.2. Testing

A stiff load frame (Terra-Tek model FX-S-33090) was used which utilizes closed-loop, servo-controlled hydraulic system with maximum axial force of 1.4 MN, and stiffness of 5×10^9 N/m. Load was measured by a sensitive load cell located in series with the sample stack, having a maximum capacity of 1000 kN and a linearity of 0.5% full scale. The axial strain cantilever set has a 10% strain range and the radial strain cantilevers have a strain range limit of 7%, with 1% linearity full scale for both sets. The samples were loaded in compression at a constant strain rate of 1×10^{-5}/s and at ambient temperature. The total volumetric strain (ε) was calculated in these tests using the sum of the component strains, i.e. $\varepsilon = \varepsilon_a + \varepsilon_{R1} + \varepsilon_{R2}$, where ε_a is axial strain, and ε_{R1} and ε_{R2} are radial strains. ε_{R1} and ε_{R2} were measured in orthogonal directions. The crack damage stress (σ_{cd}), which is the stress level at which maximum volumetric strain is attained, was determined using a plot of total volumetric strain versus axial compressive stress. Maximum volumetric strain (ε_{cd}) is the reversal point in the slope of the total volumetric strain curve (Martin and Chandler, 1994; Wong et al., 1997; Eberhardt et al., 1999). For example, axial stress versus axial, radial and volumetric strains is plotted in Fig. 1 for Beit-Meir Dolomite (sample BM-2). Reversal in the volumetric strain curve occurred at 40 MPa with a maximum volumetric strain of $\varepsilon_{cd} = 0.0362\%$. Failure of sample BM-2 occurred at uniaxial compressive strength value of $\sigma_c = 72$ MPa.

2.3. Physical and mechanical properties

The dry bulk density (ρ), initial porosity (n), and elastic constants (elastic modulus, E, and Poisson's ratio, ν) of the tested rocks are summarized in Table 1. The porosity (n) was calculated from measured values of dry bulk density (ρ) and specific gravity of solids, and ranged between 5.4% and 29%. The precision of porosity estimation is 0.1%. The values of elastic moduli range between $18{,}000 < E < 64{,}000$ MPa with an average value of 40,000 MPa. Poisson's ratio values have a range of $0.19 < \nu < 0.4$ with an average value of 0.25. The elastic modulus and Poisson's ratio were calculated using linear regression along the linear segment of the stress–strain curve.

Table 1
Density, porosity and elastic constants of studied rocks

Rock	Sample	ρ (g/cm^3)	n (%)	E (MPa)	ν
Bina Limestone	BINA-1	2.63	6.1	60,450	0.23
	BINA-2	2.36	15.7	34,400	0.25
	BINA-5	2.42	13.6	38,700	0.24
	BINA-6	2.51	10.4	24,800	0.27
	BINA-7	2.4	14.3	25,000	0.2
	TH5-15	2.42	13.6	37,700	0.27
Aminadav Dolomite	AD-43	2.65	5.4	64,000	0.27
	AD-5	2.62	5.8	56,000	0.37
	AD-15	2.19	20.9	29,000	0.26
	AD-80	2.62	6.4	58,500	0.28
	AD-83	2.37	15.4	18,000	0.25
Yagur Dolomite	CA-3541	2.57	8.2	54,000	0.19
	CA-5631	2.56	8.6	46,400	0.21
	CA-5671	2.33	16.8	35,500	0.19
Sorek Dolomite	BZ5-16	2.31	17.5	24,300	0.22
	BZ2-61A	2.42	13.6	22,300	0.2
	BZ2-35A	2.36	15.7	16,200	0.26
Beit-Meir Dolomite	BM-2	2.32	17.1	38,100	0.4
	BM-3	1.98	29	21,400	0.215
Nekarot Limestone	GN2-1B	2.48	8.3	47,000	0.23
	GN2-4A	2.43	10.1	44,600	0.25
	GN2-5B	2.49	7.6	48,600	0.25
	GN3-2A	2.45	9.3	44,800	0.24
	GN3-2C	2.42	10.4	44,400	0.25
	GN3-3A	2.47	8.4	49,000	0.28

Legend: ρ = dry bulk density, n = porosity, E = elastic modulus, ν = Poisson's ratio.

Crack damage stress (σ_{cd}), uniaxial compressive strength (σ_c), and maximum total volumetric strain (ε_{cd}) are summarized in Table 2. Crack damage stress ranges between $22 < \sigma_{cd} < 274$ MPa, uniaxial compressive strength values have a range of $32 < \sigma_{cd} < 274$ MPa, and maximum volumetric strain (ε_{cd}) varies from 0.0362% to 0.236%.

2.4. Petrographic description

The petrographic analysis was performed using petrographic and scanning electron microscopes. Grain size distribution, percent calcite, porosity and nature of contacts between grains were analyzed. SEM analysis was performed on thin sections of size 3×5 mm, which were cut from near the failure zone in each sample after loading. The mean grain size values range between $6 < d_m < 50$ μm and $7 < d_m < 12$ μm for dolomites and limestones, respectively. Detailed petrographic description (including micrographs and grain size distribution curves, proportion between the mosaic textures, etc.) of the studied rocks is presented elsewhere (Hatzor et al., 1997; Hatzor and Palchik, 1997, 1998; Palchik and Hatzor, 2000).

Table 2
Stress levels and maximum volumetric strain of studied rocks

Rock	Sample	ε_{cd} (%)	σ_{cd} (MPa)	σ_c (MPa)
Bina Limestone	BINA-1	0.142	170	187
	BINA-2	0.136	77	77
	BINA-5	0.1	80	80
	BINA-6	0.12	65	89
	BINA-7	0.132	64	64
	TH5-15	0.095	78	84
Aminadav Dolomite	AD-43	0.21	274	274
	AD-5	0.06	85	98
	AD-15	0.09	57	67
	AD-80	0.134	174	174
	AD-83	0.07	43	62
Yagur Dolomite	CA-3541	0.149	174	174
	CA-5631	0.168	105	186
	CA-5671	0.14	60	60
Sorek Dolomite	BZ5-16	0.162	64	78
	BZ2-61A	0.137	50	86
	BZ2-35A	0.084	22	32
Beit-Meir Dolomite	BM-2	0.0362	40	72
	BM-3	0.089	46	46
Nekarot Limestone	GN2-1B	0.236	177	184
	GN2-4A	0.165	141	141
	GN2-5B	0.197	162	162
	GN3-2A	0.161	150	150
	GN3-2C	0.186	163	163
	GN3-3A	0.171	175	178

Legend: ε_{cd} = maximum total volumetric strain, σ_{cd} = crack damage stress, σ_c = uniaxial compressive strength.

3. The effect of microstructural parameters

3.1. Typical axial stress–volumetric strain curves

Typical stress–volumetric strain curves of uniaxial compression tests for two limestone samples (BINA-1 and BINA-6) and two dolomite samples (AD-43 and AD-15) are presented in Figs. 2 and 3, respectively. The uniaxial compressive strength is represented by point (A), whereas crack damage stress is represented by point (B). In Fig. 2, sample BINA-1 exhibits crack damage stress (σ_{cd}) of 170 MPa, 2.62 times greater than the σ_{cd} of sample BINA-6 (65 MPa). The crack damage stress (σ_{cd}) is attained at 0.91 σ_c and 0.73 σ_c in samples BINA-1 and BINA-6, respectively. The stronger sample (BINA-1, $E = 60{,}450$ MPa, $n = 6.07\%$) exhibits higher elastic modulus (E) and lower porosity (n) with respect to the weaker sample (BINA-6, $E = 24{,}800$ MPa, $n = 10.36\%$). In Fig. 3 crack damage stress (σ_{cd}) is attained at 1.0 σ_c and 0.85 σ_c in samples AD-43 and AD-15, respectively. Sample AD-43, with an extremely high level of $\sigma_{cd} = 274$ MPa, exhibits very high elastic modulus ($E = 64{,}000$ MPa) and relatively low porosity ($n = 5.4\%$). On the other hand, σ_{cd} of sample AD-15 is relatively low (57 MPa) and this sample exhibits low elastic modulus ($E = 29{,}000$ MPa) and relatively high porosity ($n = 20.9\%$). It is clear that the difference between σ_{cd} values of samples BINA-1 and BINA-6, AD-43 and AD-15 is due to the differences in matrix stiffness and porosity. In general, a lower porosity and higher elastic modulus corresponds to a higher value of σ_{cd}.

The relationships between crack damage stress (σ_{cd}), elastic modulus (E), and porosity (n) are discussed below.

3.2. Effect of matrix stiffness

The relationship between elastic modulus (E) and crack damage stress (σ_{cd}) is shown in Fig. 4 for all

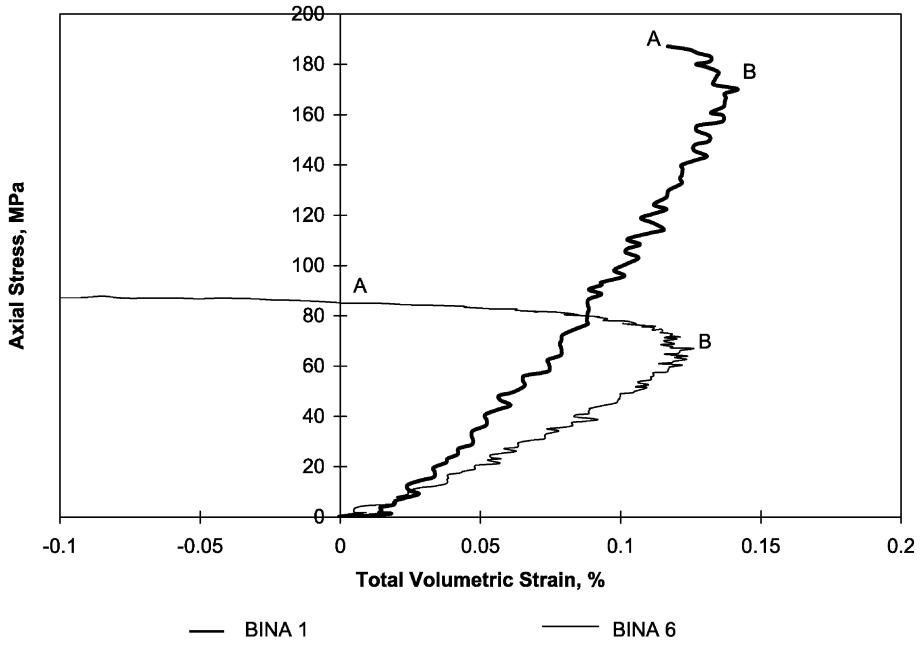

Fig. 2. Two stress–volumetric strain curves for limestone samples (A—peak strength; B—crack damage stress).

samples. It can be seen that crack damage stress increases with increasing elastic modulus (E). Using the least squared fit method, we found that the relation between σ_{cd} and E follows power ($R^2 = 0.7596$), exponential ($R^2 = 0.7433$) and second-order polynomial ($R^2 = 0.7569$) laws. Elastic modulus (E), which is

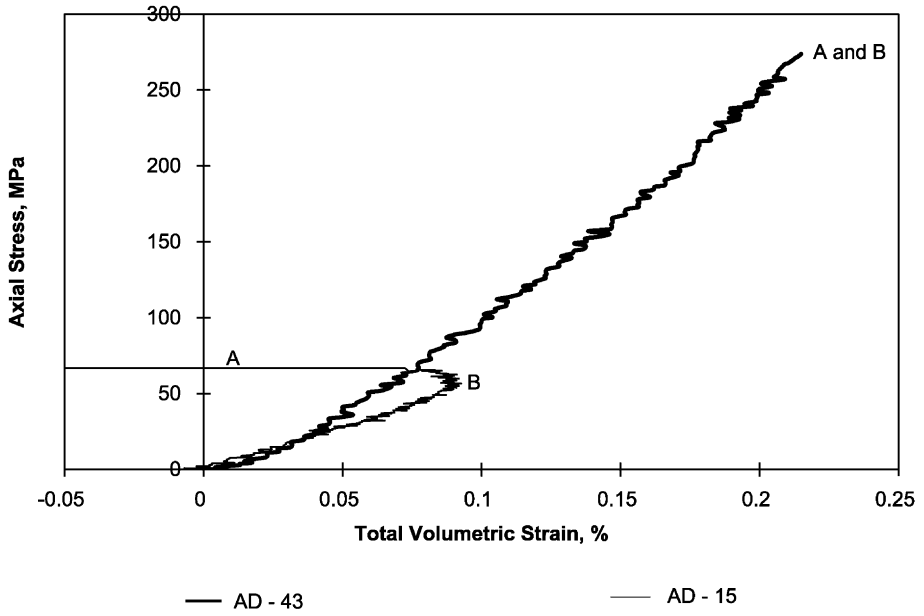

Fig. 3. Two stress–volumetric strain curves for dolomite samples (A—peak strength; B—crack damage stress).

measured along the linear segment of the stress–strain curve, is a manifestation of rock stiffness which influences rock strength as discussed by Hatzor and Palchik (1998), Palchik (1999), Palchik and Hatzor (2000). Rock stiffness in granular rocks depends on the length of stiff grain to grain contacts and on the number of contacts per grain. David et al. (1998) and Digby (1981) have shown that granular rocks are stiffer when the contact length is larger.

3.3. Effect of porosity

Fig. 5 illustrates the relationship between porosity (n) and crack damage stress (σ_{cd}) for all samples. Clearly, crack damage is inversely related to porosity, and this result confirms our assumption that initial pores are significant stress concentrators. Similar pronounced effects of porosity, but with respect to uniaxial compressive strength, were obtained by Farquhar et al. (1994), Dunn et al. (1973), Hoshino (1974) and Vernik et al. (1973) for heterogeneous sandstones, and by Dearman et al. (1978) for dolerite and granite. These studies have shown exponential relationships between uniaxial compressive strength and porosity. Results obtained through this study, however, suggest that the relationship $\sigma_{cd} - n$ may be better described by a second-order polynomial law ($R^2 = 0.6801$).

4. An empirical model for crack damage stress

4.1. Combinations of dependencies σ_{cd}–E and σ_{cd}–n

It was shown in the preceding section that the relationship between σ_{cd} and E (Fig. 4) can be described by a power, exponential or second-order polynomial law, since the obtained values of squared regression coefficients do not differ significantly ($R^2 = 0.7596$, 0.7433 and 0.7569, respectively). For this study, power ($\sigma_{cd} = k_1 E^{k_2}$) and exponential ($\sigma_{cd} = k_1 \exp(k_2 E)$) laws were chosen since these laws are simpler than the second-order polynomial law. It was also found that the $\sigma_{cd} - n$ relationship (Fig. 5) best follows a second-order polynomial law ($R^2 = 0.6801$), i.e. $\sigma_{cd} = k_3 n^2 - k_4 n + k_5$. In these functions, $k_1, \ldots, k_5$ are empirical coefficients. However, examination of the above-mentioned combinations using power or exponential functions for $\sigma_{cd} = f(E)$ and a second-order polynomial function for $\sigma_{cd} = f(n)$, does

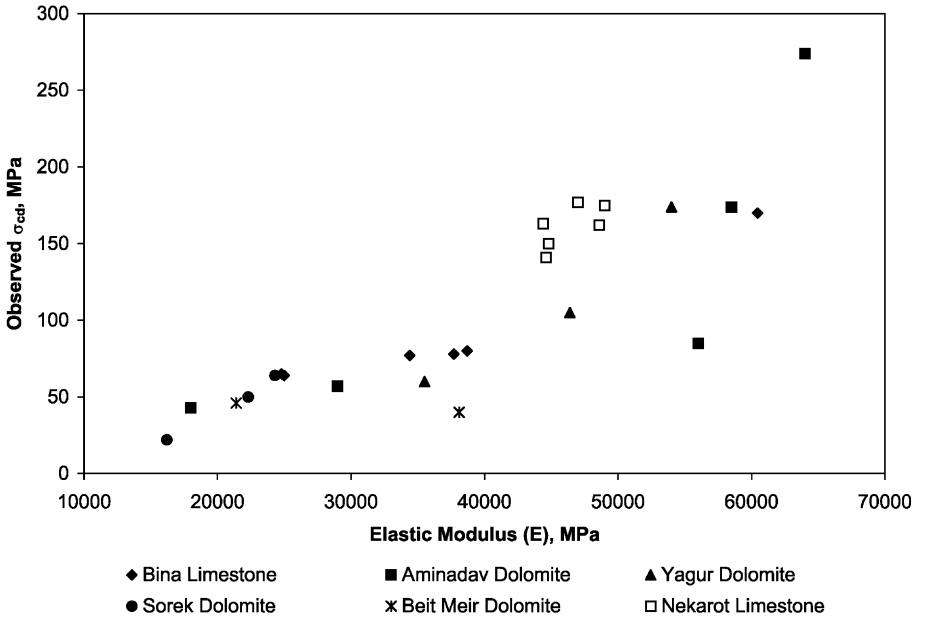

Fig. 4. Correlation between elastic modulus and crack damage stress.

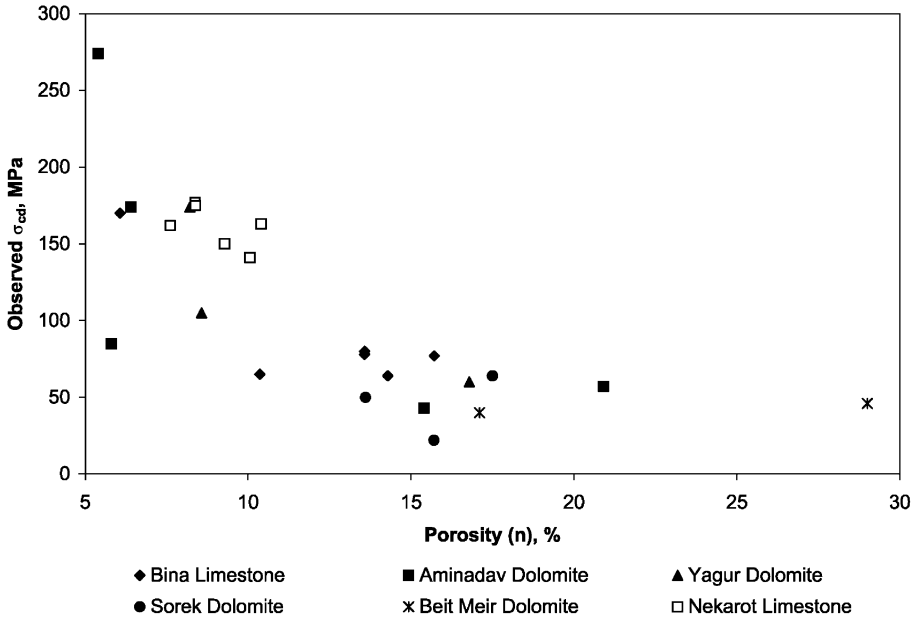

Fig. 5. Relationship between porosity and crack damage stress.

not lead to an explicit form of a composite model $\sigma_{cd}=f(E, n)$ with a reasonable regression coefficient. We obtained the best fit $\sigma_{cd}=E^{k1}/(k_2n^2-k_3n+k_4)$ with a weak squared regression coefficient ($R^2=0.73$); such a composite model requires four empirical coefficients ($k_1=0.8$; $k_2=0.3$, $k_3=2.3$ and $k_4=26.7$).

This fact suggests that an empirical model for $\sigma_{cd}=f(E, n)$ cannot be developed based exclusively on the correlation between σ_{cd}, E and n.

4.2. Model $\sigma_{cd}=f(E, n/\varepsilon_{cd})$

Since σ_{cd} was shown to be directly related to the elastic modulus (E) and inversely related to porosity (n), we can try to use the ratio (E/n) for simple description of the combined influence of E and n:

$$\sigma_{cd}=f\left(\frac{E}{n}\right). \quad (1)$$

Porosity, $n=V_p/V$ is a measure of void space (pores and open cracks) and presents the ratio between void space (V_p) and bulk volume (V). The latter is the initial volume of the sample before loading, and therefore it does not reflect the change in volume due to compression. We believe that it would be appropriate to use the ratio between the volume of voids and change in bulk volume due to compression since such ratio reflects the mechanical behavior of the rock matrix. This ratio is given by $n/\varepsilon_{cd}=(V_p/V)/(V_c/V)=V_p/V_c$, where V_c is the maximum decrease in sample volume (maximum compaction of sample), which is attained at the reversal point in the slope of total volumetric strain. Thus, n/ε_{cd} is the ratio between the volume of voids and the maximum compaction of rock sample. If we insert the n/ε_{cd} instead of n in expression (1), we obtain an implicit form:

$$\sigma_{cd}=f\left(E\frac{\varepsilon_{cd}}{n}\right). \quad (2)$$

In order to determine the explicit form of Eq. (2), values of σ_{cd} were linked with values of $E(\varepsilon_{cd}/n)$ for each of the 25 samples. We examined linear, power, exponential, logarithmic, and second-order polynomial correlations between σ_{cd} and $E(\varepsilon_{cd}/n)$ using the least squares fit method. As a result, we obtained a

linear law between $E(\varepsilon_{cd}/n)$ and crack damage stress:

$$\sigma_{cd} = aE\frac{\varepsilon_{cd}}{n} + b \quad (3)$$

where σ_{cd} is crack damage stress (MPa), ε_{cd} is maximum total volumetric strain (%), n is porosity (%), E is elastic modulus (MPa), a and b are empirical coefficients ($a=0.08$ for all dolomite formations, 0.07 for Bina Limestone, and 0.1 for Nekarot Limestone; $b=40$ and 50 MPa for $n>15\%$ and $n<15\%$, respectively). Coefficient b is the minimum value of σ_{cd} when porosity is at its maximum and the elastic modulus is at its minimum.

It can be seen from Table 2 that the minimum value of σ_{cd} (i.e. coefficient b) in the tested samples achieves 40–50 MPa, excluding an initially cracked sample BZ2-35A (Sample BZ2-35A contained several evident fractures and therefore its strength was very low: $\sigma_{cd}=22$ MPa, $\sigma_c=32$ MPa).

In Fig. 6, comparison between calculated (Eq. (3)) and observed crack damage stress for all samples (excluding sample BZ2-35A) shows that the obtained linear squared regression coefficient ($R^2=0.9329$) is good.

Eq. (3) is an empirical model for σ_{cd} in terms of E and the ratio ε_{cd}/n. However, the practical application of Eq. (3) is impossible since there are two unknown quantities (σ_{cd} and ε_{cd}). For calculation of σ_{cd} and ε_{cd}, it is necessary to obtain an additional equation for these unknown quantities.

4.3. Model $\sigma_{cd}=f[E/(1-2\nu),\varepsilon_{cd}]$

In order to obtain an additional relationship for σ_{cd} and ε_{cd}, we generalize the ratio $\sigma_{cd}/\varepsilon_{cd}$ with respect to the elastic expression $E/(1-2\nu)$, which is often used in theory of elasticity. For example, Martin and Chandler (1994) and Hatzor and Palchik (1997) have used this elastic expression to calculate the ratio between crack initiation stress and volumetric strain at crack initiation. It is established in this study that the ratio $\sigma_{cd}/\varepsilon_{cd}$ increases polynomially with increasing value of $E/(1-2\nu)$ in all samples. Hence, the additional equation has the following form:

$$\frac{\sigma_{cd}}{\varepsilon_{cd}} = c\frac{E}{1-2\nu} - d\left(\frac{E}{1-2\nu}\right)^2 \quad (4)$$

where c and d are empirical coefficients (for the studied rocks $c=0.0124$ and $d=3e-08$).

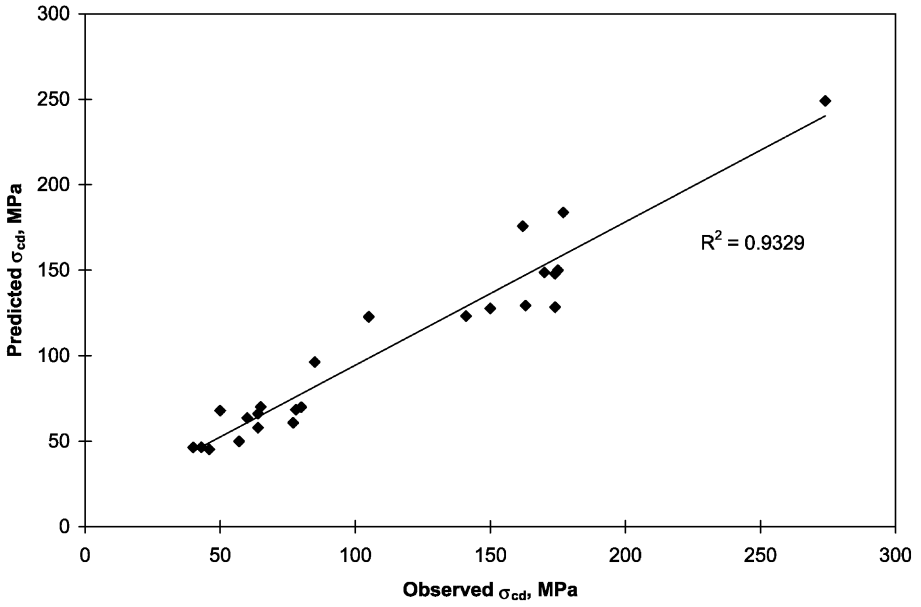

Fig. 6. Comparison between calculated (Eq. (3)) and observed σ_{cd} ($R^2=0.9329$).

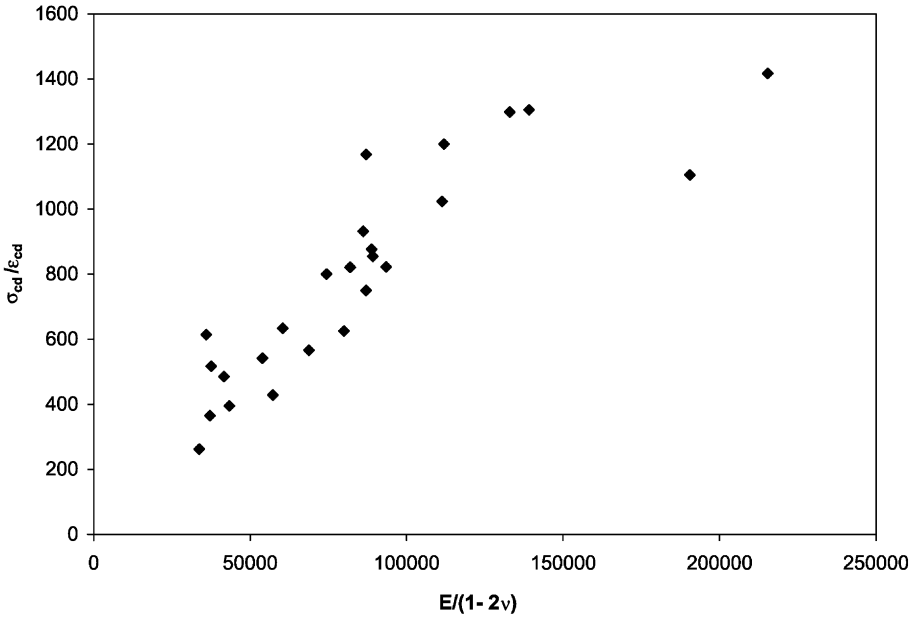

Fig. 7. Polynomial correlation between $\sigma_{cd}/\varepsilon_{cd}$ and $E/(1-2\nu)$ in all samples studied.

The ratio $\sigma_{cd}/\varepsilon_{cd}$ in each of the 25 unconfined compression tests is plotted against $E/(1-2\nu)$ in Fig. 7, where a reasonable polynomial correlation ($R^2=0.835$) is obtained.

4.4. The final model $\sigma_{cd}=f[E/(1-2\nu), n]$

The solution of the system of Eqs. (3) and (4), with respect to σ_{cd} provides the final model for crack damage stress (σ_{cd}) in terms of porosity (n), elastic modulus (E), Poisson's ratio (ν) and three empirical coefficients:

$$\sigma_{cd} = b\left[1+\frac{1}{\frac{n}{1-2\nu}\left(K_1-\frac{K_2E}{1-2\nu}\right)-1}\right] \quad (5)$$

where b, K_1 and K_2 are empirical coefficients: $b=40$ and 50 MPa for porosity $n>15\%$ and porosity $n<15\%$, respectively; $K_1=c/a$ and $K_2=d/a$ are presented in Table 3.

The test data are plotted against our model prediction of σ_{cd} (Eq. (5)) for the 24 tested specimens in Fig. 8. The squared linear regression coefficient in Fig. 8 is reasonable ($R^2=0.8314$).

The root mean square error between observed and predicted crack damage stress (for 24 samples involved in predicting σ_{cd}) is 18.8%, i.e. this error is less than 20% that which is permissible for engineering computation. The root mean square error between observed values and the predicted values has been calculated as follows:

$$\Delta = \sqrt{\frac{\sum_{i=1}^{n=24}\left(\sigma_{cdi}^{o}-\sigma_{cdi}^{P}\right)^2}{n-1}}100 \quad (6)$$

where $i=1,2,3,\ldots,n$ is the number of tested samples; $\sigma_{cdi}{}^{o}$ is the observed value of σ_{cd} in ith

Table 3
Empirical coefficients in studied rocks

Rock	Formation	K_1	K_2
Dolomite	Aminadav	0.155	3.75e-07
	Yagur		
	Sorek		
	Beit-Meir		
Limestone	Bina	0.177	4.28e-07
	Nekarot	0.124	3e-07

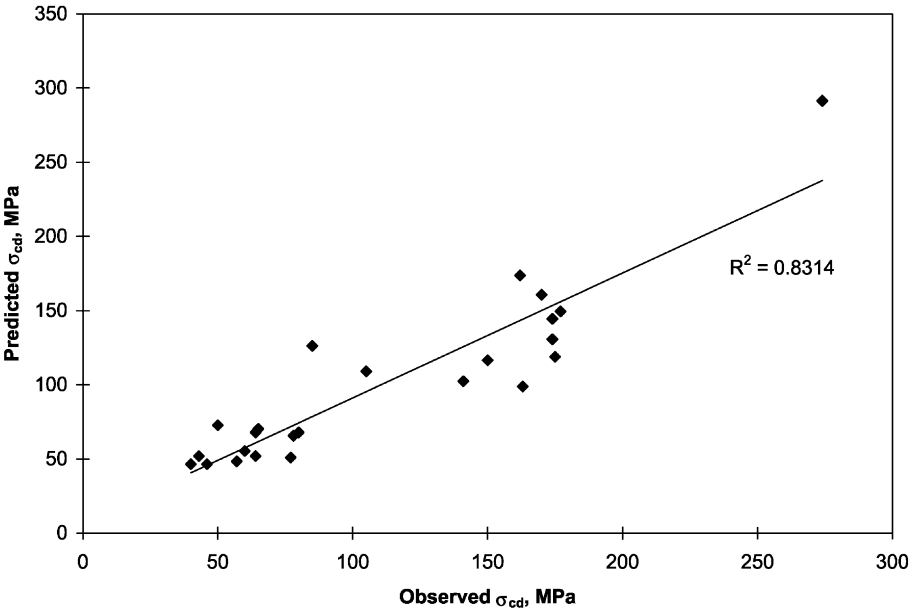

Fig. 8. Predictive capability of the final model for σ_{cd} (Eq. (5)) ($R^2 = 0.8314$).

sample; σ_{cdi}^{p} is the predicted value of σ_{cd} in *i*th sample.

5. Discussion

Our proposed model for crack damage stress (Eq. (5)) consists of three mechanical and physical variables: elastic modulus, Poisson's ratio and porosity. Consider the relation between variables E and n in all samples shown in Fig. 9. It is clearly seen in Fig. 9 that the elastic modulus (E) increases with decreasing porosity (n). Probably, the length of grain to grain contacts and the number of contacts per grain, a textural feature which directly influences rock stiffness (David et al., 1998; Digby, 1981), increases with decreasing void space. Note, however, that the dependence $E-n$, which best follows a second-order polynomial law, has a relatively weak squared regression coefficient ($R^2 = 0.7497$). This observation suggests that the elastic modulus (stiffness) only partly depends on porosity. This is not surprising since mosaic texture, mineralogical composition and pore types also influence the nature of contacts between grains in heterogeneous dolomites and limestones (Roehl and Choquette, 1985; Mazullo et al., 1992; Durrast and Siegesmund, 1999). Hence, there is no simple explicit dependence (with reasonable regression coefficients) between E and n, which can be inserted in the proposed model (Eq. (5)).

Fig. 10 presents how the predicted crack damage stress (σ_{cd}) varies with elastic modulus (E) and porosity (n) when $\nu_{aver} = 0.25$, $b_{aver} = 45$ MPa, $K_{1\,aver} = 0.154$ and $K_{2\,aver} = 3.71e-07$. The values of elastic modulus and porosity plotted on the vertical axes in Fig. 10 are mutually dependent, and when porosity on the right vertical axis decreases from 21.5% to 5.5%, the elastic modulus on the left vertical axis increases from 18,000 to 64,000 MPa. The curve $\sigma_d = f(E, n)$ was plotted using Eq. (5). Note that the correspondence between the values of E and n on the vertical axes in Fig. 10 is an approximate average, as it was determined by polynomial interpolation and because no explicit function between E and n was found as discussed. This correlation is only used to show the expected trend and is not to be taken as precise.

When porosity decreases and elastic modulus increases simultaneously, the crack damage stress rapidly increases and approaches its maximum value. On the other hand, when porosity increases and elastic

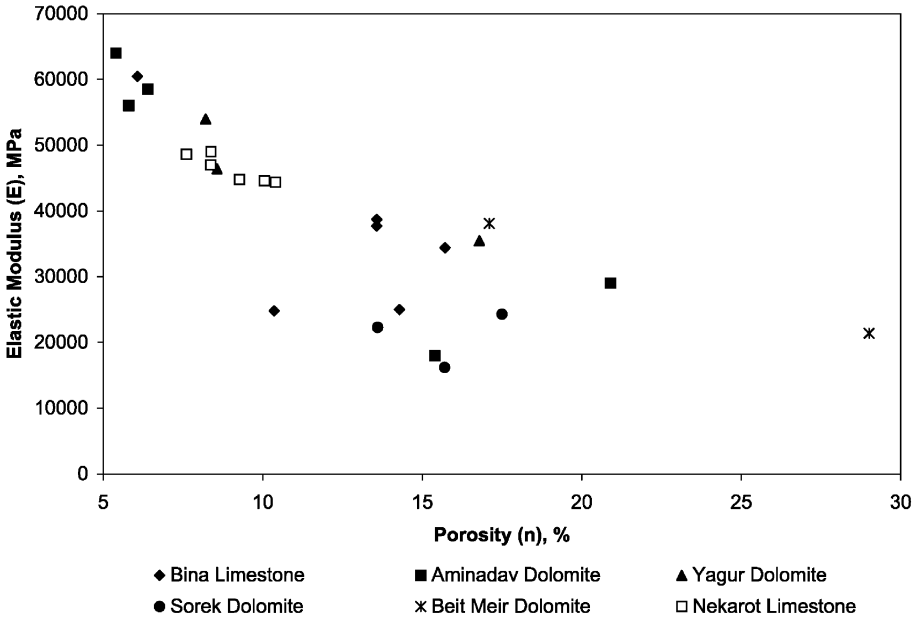

Fig. 9. Influence of porosity (n) on elastic modulus (E) in the studied samples.

modulus decreases simultaneously, the crack damage stress rapidly decreases and approaches its minimum value.

Our empirical model (Eq. (5)), can be used to predict crack damage stress (σ_{cd}) in the studied limestone and dolomite formations as long as the elastic

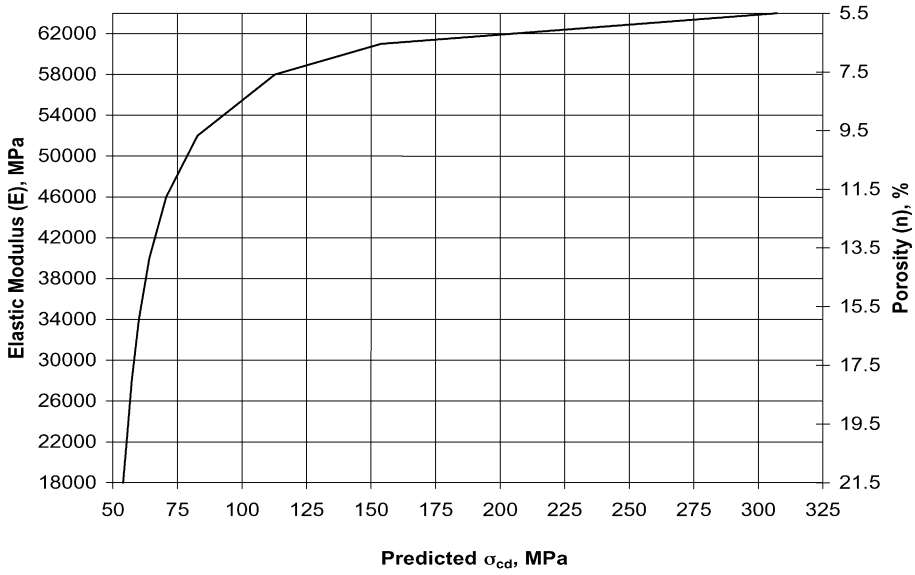

Fig. 10. Empirical model prediction for the influence of porosity and elastic modulus on crack damage stress.

parameters E and ν and the porosity (n) are known. The advantage of our model is that it predicts the crack damage stress, but actual measurements of volumetric strain during loading are not necessary, provided that the elastic constants of the material and the porosity are known. This advantage can be utilized in the following cases:

- When strain output is measured during loading at a very small data acquisition rate, at conventional rock testing laboratories, which perform routine tasks for the industry. Slow acquisition rate may be sufficient to determine the elastic modulus and Poisson's ratio quite accurately because of a substantial linear elastic range in the studied rocks. However, the reversal point in the volumetric strain output may be overlooked in slow data acquisition modes in the non-linear region. Moreover, the transition from decrease to increase in total volume is often smooth and difficult to locate. For example, see volumetric strain for Beit-Meir Dolomite (sample BM-2) in Fig. 1, where $\sigma_{cd} = 40$ MPa can be obtained using very rapid data acquisition with acquisition time interval smaller than 3 s. This testing capability is often available at university research facilities, but is rare in the industry.
- The elastic constants and the porosity for the studied lithologies are already known from previous testing.
- The porosity is known and the static elastic constants are estimated from dynamic (e.g. ultrasonic) tests.

In all the cases mentioned above, we can calculate the crack damage stress using E, ν and n, and three empirical coefficients: $b = 45-50$ MPa, K_1, and K_2 (Table 3). In the proposed model (Eq. (5)) grain size is omitted and the elaborate laboratory research necessary to determine grain size distribution using petrographic or scanning electron microscopes is not required.

The crack damage stress is indeed sensitive to the value of the empirical coefficients. For example, at $n = 10\%$, $\nu = 0.25$ and $E = 35000$ MPa, σ_{cd} (Eq. (5)) would be 81.7, 73.8 and 97.17 MPa for dolomites, Bina Limestone and Nekarot Limestone, respectively, depending on the value of the empirical constants. The change in empirical coefficient values may lead to a change in σ_{cd} from 9.7% to 24 %.

We have only one limestone sample (Yanuah Limestone), which was not involved in development of our model (Eq. (5)). We can use sample Yanuah 1 in order to validate our model. Sample Yanuah 1 exhibits $E = 37800$ MPa, $\nu = 0.4$, $n = 6.8\%$ and $\sigma_{cd} = 0.55\ \sigma_c = 60$ MPa, which were determined experimentally in our laboratory. According to model (Eq. (5)) (using $K_1 = 0.177$ and $K_2 = 4.28e-07$ for Bina Limestone), the predicted $\sigma_{cd} = 72$ MPa. Thus, the relative error is $[(72-60)/72]100 = 16.7\%$. Note, that we used K_1 and K_2 for Bina Limestone since these values for Yanuah limestone are unknown and cannot be determined using only one sample, rather at least three samples of the Yanuah Limestone are needed. Verification of K_1 and K_2 for Yanuah Limestone will allow to decrease the error between measured and predicted σ_{cd}.

In order to generalize this model to other heterogeneous limestones and dolomites, the values of E, ν, σ_{cd} and n must be determined experimentally using a relatively small number of tests with advanced testing facilities. Then, the values of the empirical coefficients must be turned over to industrial laboratories for further use.

The predictive capability of the proposed composite dependence $\sigma_{cd} = f(E,\ n$ and $\nu)$ is reasonable (linear regression coefficient $R^2 = 0.8314$). The proposed empirical model is expected to be valid for dolomites and limestones for the following range of physical and mechanical parameters: $5.4 < n < 29\%$, $18{,}000 < E < 64{,}000$ MPa and $0.19 < \nu < 0.4$.

6. Conclusion

The work presented in this paper suggests that the elastic stiffness (as defined by the elastic constants E, ν) and porosity (n) influence the onset of dilation, otherwise known as the "crack damage stress". It is argued that σ_{cd} is a composite function of porosity and the elastic stiffness. The crack damage stress at which total volumetric strain attains maximum, is partly related to elastic modulus and inversely related to porosity. When porosity is decreased and elastic modulus is increased, the crack damage stress increases from its minimum to maximum value. Using the proposed model it concluded that the elastic constants (E, ν) and the bulk porosity (n) would be sufficient to calculate the crack damage stress (σ_{cd}) for the studied heterogeneous dolomites and limestones.

Acknowledgements

Parts of this work have been funded by Geoprospect Jerusalem (contract 1888/95) and Oil Products Pipelines (contract C.97520187) and their support is hereby acknowledged. We thank Dr. E. Eberhardt and an anonymous reviewer for their critical review of paper. Their comments and recommendations improved the quality of the manuscript.

References

Al-Harthi, A.A., Al-Amri, R.M., Shehata, W.M., 1999. The porosity and engineering properties of vesicular basalt in Saudi Arabia. Eng. Geol. 54, 313–320.

Bieniawski, Z.T., 1967. Mechanism of brittle fracture of rock: Part I—Theory of the fracture process. Int. J. Rock Mech. Min. Sci. Grommet. Amstar. 4, 395–406.

Brace, W.F., 1978. Volume changes during fracture and frictional sliding: a review. PAGEOGH 116, 603–614.

Brady, B.H.G., Brown, E.T., 1993. Rock Mechanics for Underground Mining, 2nd edn. Chapman & Hall, London, 571 pp.

David, C., Menendez, B., Bernabe, Y., 1998. The mechanical behavior of synthetic sandstone with varying cement content. Int. J. Rock Mech. Min. Sci. Geomech. Abstr. 35 (6), 759–770.

Dearman, W.R., Baynes, E.J., Irfan, T.Y., 1978. Engineering grading of weathered granite. Eng. Geol. 12, 345–374.

Digby, P.J., 1981. The effective elastic moduli of porous granular rocks. J. Appl. Mech. 48, 803–808.

Dunn, D.E., LaFountain, L.J., Jackson, R.E., 1973. Porosity dependence and mechanism of brittle fracture in sandstones. J. Geophys. Res. 78, 2403–2417.

Durrast, H., Siegesmund, S., 1999. Correlation between rock fabrics and physical properties of carbonate reservoir rocks. Int. J. Earth Sci. 88 (3), 392–408.

Eberhardt, E., Stead, D., Stimpson, B., 1999. Quantifying progressive pre-peak brittle fracture damage in rock during uniaxial compression. Int. J. Rock Mech. Min. Sci. Geomech. Abstr. 36, 361–380.

Farquhar, R.A., Sowervile, J.M., Smart, B.G.D., Heriot-Watt, U., 1994. Porosity as a geomechanical indicator: an application of core and log data in rock mechanics. European Petroleum Conference. Society of Petroleum Engineers, London, pp. 481–489 (SPE 28853).

Fredrich, J.T., Evans, B., Wong, T.F., 1990. Effect of grain size on brittle and semibrittle strength: implications for micromechanical modeling of failure in compression. J. Geophys. Res. 95, 10,907–10,920.

Griffith, A.A., 1921. The phenomena of rupture and flow in solids. Philos. Trans. R. Soc. London, Ser. A 221, 163–197.

Hatzor, Y.H., Palchik, V., 1997. The influence of grain size and porosity on crack initiation stress and critical flaw length in dolomites. Int. J. Rock Mech. Min. Sci. Geomech. Abstr. 34 (5), 805–816.

Hatzor, Y.H., Palchik, V., 1998. A microstructure-based failure criterion for Aminadav Dolomites. Int. J. Rock Mech. Min. Sci. Geomech. Abstr. 35 (6), 797–805.

Hatzor, Y.H., Zur, A., Mimran, Y., 1997. Microstructure effect on microcracking and brittle failure of dolomites. Tectonophysics 281, 141–161.

Hoshino, K., 1974. Effect of porosity on strength of clastic sedimentary rock. Proc. 3rd Cong. Int. Soc. Rock. Mech., Denver, CO, vol. 1. Balkema, Rotterdam, pp. 511–516.

Logan, J.M., 1987. Porosity and brittle–ductile transition in sedimentary rocks. In: Banavar, J.R., Koplik, J., Winker, K.W. (Eds.), Physics and Chemistry of Porous Media IIAIP Conf. Proc. American Institute of Physics, New York, pp. 229–242.

Lumb, P., 1983. Engineering properties of fresh and decomposed igneous rocks from Hong Kong. Eng. Geol. 19, 81–94.

Martin, C.D., Chandler, N.A., 1994. The progressive fracture of Lac du Bonnet Granite. Int. J. Rock Mech. Min. Sci. Geomech. Abstr. 31 (6), 643–659.

Mazullo, S.J., Chilingarian, G.V., Bissell, H.J., 1992. Carbonate rock classification. Carbonate Reservoirs Characterization: a Geological-Engineering Analysis. Part 1. Elsevier, Amsterdam, pp. 59–108.

Olsson, W.A., 1974. Grain size dependence of yield stress in marble. J. Geophys. Res. 79, 4859–4862.

Palchik, V., 1999. Influence of porosity and elastic modulus on uniaxial compressive strength in soft brittle porous sandstones. Rock Mech. Rock Eng. 32 (4), 303–309.

Palchik, V., Hatzor, Y.H., 2000. Correlation between mechanical strength and microstructural parameters of dolomites and limestones in the Judea group, Israel. Isr. J. Earth Sci. 49 (2), 65–79.

Paterson, M.S., 1978. Experimental Rock Deformation—The Brittle Field. Springer-Verlag, New York, 254 pp.

Roehl, P.O., Choquette, P.W., 1985. Introduction. Carbonate petroleum reservoirs. Springer, Berlin, pp. 1–15.

Schock, R.N., Heard, H.C., Stevens, D.R., 1973. Stress–strain behavior of a granodiorite and two graywackes on compression to 20 kilobars. J. Geophys. Res., 5922–5941.

Scott, T.E., Nielson, K.C., 1991. The effect of porosity on brittle–ductile transition in sandstones. J. Geophys. Res. 96, 405–414.

Teufel, L.W., Rhett, D.W., 1991. Geomechanical evidence for shear failure of chalk during production of the Ekofisk field. Proc. SPE 66th Annual Tech. Conf. SPE 22755, Dallas.

Vernik, L., Bruno, M., Bovberg, C., 1993. Empirical relations between compressive strength and porosity of siliclastic rocks. Int. J. Rock Mech. Min. Sci. Geomech. Abstr. 30 (7), 677–680.

Wong, R.H.C., Chau, K.T., Wang, P., 1996. Microcracking and grain size effect in Yeun Long marbles. Int. J. Rock Mech. Min. Sci. Geomech. Abstr. 33 (5), 479–485.

Wong, T.-F., David, C., Zhu, W., 1997. The transition from brittle faulting to cataclastic flow in porous sandstones: mechanical deformation. J. Geophys. Res. 102, 3009–3025.